Modeling and Optimization of Bistable Composite Laminates for Piezoelectric Actuation

David N. Betts, H. Alicia Kim and Christopher R. Bowen
Department of Mechanical Engineering, University of Bath, Bath, BA2 7AY, United Kingdom

Adaptive structures that allow large deformations under the application of a low and non-continuous energy input are gaining increasing interest in the aerospace industry. One potential mechanism of realising shape control is piezoelectric actuation of asymmetric composite laminates. This paper presents an optimization study for the design of bistable laminates for reversible snap-through enabled by two orthogonal piezoelectric layers. The formulation optimizes the load carrying capability of the structure subject to deflection and actuation limits through variation in ply orientations and laminate geometry. We find the problem to be multimodal with the multiple optima to be dependent on the loading and snap-through directions and the complex constraint boundary interactions. A reduction in the total actuation voltage is achieved through the simultaneous use of the positive and negative working ranges of the two piezoelectric layers.

I. Introduction

Asymmetric composite laminates have been considered for adaptive structures due to the relatively low power requirement to achieve large structural deformations. When laminates of this type are cured at elevated temperature the mismatch in thermal expansion coefficients between individual plies results in a thermally induced strain. This leads to a curved deformation of the laminate. Under certain geometric conditions the thermal distortion can lead to two stable configurations with approximately cylindrical curvatures. Figure 1 shows a square $[0/90]_T$ laminate with two stable shapes of equal curvature in opposite directions. A state change from one stable state to another is achievable by applying an in-plane strain, resulting in a large out-of-plane displacement which does not require continuous energy input to be maintained.

The stable shapes of asymmetric laminates of general layup have been extensively studied using a Rayleigh-Ritz approach to minimizing the total strain energy of the laminate (Dang and Tang, 1986; Jun and Hong, 1990; Dano and Hyer, 1998). These numerical models have been further developed to include smart actuation to induce snap-through behavior. Schultz, Wilkie and Bryant (2007) investigated reversible actuation of a two-ply laminate using two orthogonal piezoelectric layers, limited to ply orientations of 0˚ and 90˚. A comparison with experimental observations demonstrated that the modeling captured the general response of the shape transition. However, the required voltage for actuation was greatly under-estimated and was outside the recommended working range of the piezoelectric material. Ren (2008) incorporated a single piezoelectric layer into an existing static model (Dano and Hyer, 1998) for shape control of laminates of general arbitrary layup (non-[0/90]), including a comparison with finite element analysis results. It was shown that for laminates of arbitrary layup a single piezoelectric actuator can be used to both control the laminate displacements and the direction of principal curvature. The analytical model compared well with finite element predictions, with some divergence in results when the voltage applied to the piezoelectric was increased. Dano and Hyer (1996) modeled an applied in-plane force arranged above the surface of the laminate on mechanical supports to induce snap-through of a $[0/90]_T$ laminate. Predictions of the force required for actuation compared very well with experimental results. This work

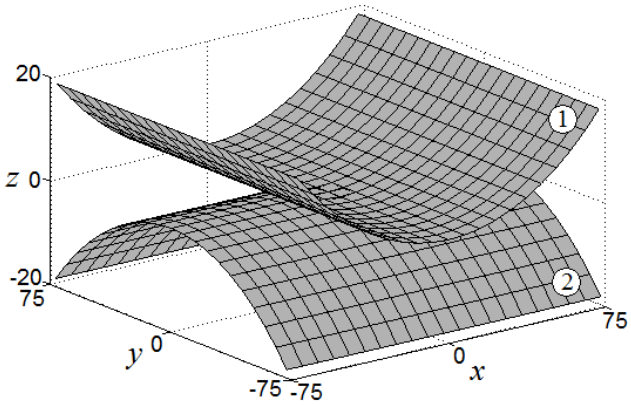

Figure 1. Two stable shapes of a square $[0/90]_T$ laminate

was later extended (Dano and Hyer, 2003) to the use of shape memory alloy (SMA) wires to generate the in-plane force in place of the mechanical force. Numerical predictions showed reasonable correlation with experiment, however, the need for the bridge-like supports can be cumbersome for practical application. Hufenbach, Gude and Kroll (2002) investigated embedding SMA wires in the laminate structure to initiate snap-through. An experimental prototype using NiTi wires was developed to demonstrate reversible snap-through. However, the transition response time for SMA materials is generally slow and the method does not offer fine shape control. Kim et al. (2010) used a combination of an SMA and a piezoelectric patch to demonstrate the reversible snap-through of a bistable cantilever. The approach used a piezoelectric patch to generate a rapid snap-through with a fine degree of control, and a slow but high strain SMA actuation to reverse the state change.

One common criticism of the asymmetric laminate adaptive structure concept is their inherent compliance and poor load carrying capability (Betts, Kim and Bowen, 2011). In order to induce a snap-through state-change using a piezoelectric actuator with a low voltage input, the stiffness must be low. This means that normal operating loads have the potential to induce an undesired state-change. The structural requirement to resist the normal operating loads and a low power requirement to induce and control the state-change are therefore, conflicting. Betts, Kim and Bowen (2011) attempted to address this issue by tailoring the composite layups to maximize the bending stiffness in one direction (in the direction of normal operating load) whilst minimizing the bending stiffness in another direction (in the direction of actuation). The numerical study showed that the stiffness in the loading direction can be five times greater than the stiffness in the actuation direction. This shows that the conflicting load carrying capability and actuation requirements may be resolved by exploiting the directional stiffness of composite lamintes.

In this paper we consider the design of asymmetric layup laminates with two orthogonal piezoelectric layers. We address the issue of unwanted state-change by optimizing for maximum bending stiffness in a chosen loading direction through variation in laminate edge length, ply thicknesses and ply orientations. To allow for the conflicting requirement of high bending stiffness and low voltage snap-through we make use of the directional stiffness properties of composites. The problem is constrained by a minimum deflection requirement and maximum actuation voltage. The following section defines the configuration of an actuated bistable composite which is considered in this paper. The optimization formulation and solution methodology are then outlined, followed by some numerical results for the design of a four-ply laminate. Finally a second optimization problem is applied to reduce the total voltage requirement for reversible actuation through the simultaneous use of the positive and negative voltage ranges of the two orthogonal piezoelectric layers.

II. Design Problem

In this section we introduce a design optimization formulation for a piezoelectrically actuated bistable composite. We consider a laminate of orthogonal layup with two shapes of equal and opposite curvature by applying the following design rules, Figure 2:

1. Two piezoelectric layers on the top and bottom surfaces of the laminate 90˚ apart.
2. An even number of plies, with pairs of plies about the laminate midplane 90˚ apart.
3. Square edge lengths, L, for both the piezoelectric layers and composite laminate.
4. Equal thicknesses, t_p, for both piezoelectric layers.
5. Equal ply thicknesses about the laminate midplane, $t_1, t_2 \ldots t_n$.
6. Each ply is made from the same material.

This laminate configuration is selected for two reasons. Firstly, it allows for the maximum deflection between the two states while providing scope for tailoring the directional stiffness properties. Secondly, the piezoelectric layers are positioned orthogonal to each other to align with the orthogonal major curvatures of the two stable cylindrical states.

In this paper we focus on the design of a four-ply laminate for illustrative purposes. This stacking sequence can be defined in terms of the first and second ply orientations, θ_1 and θ_2, and the top piezoelectric orientation θ_{p1}. However, the modeling in this paper is applicable to any even number of plies meeting the above design rules.

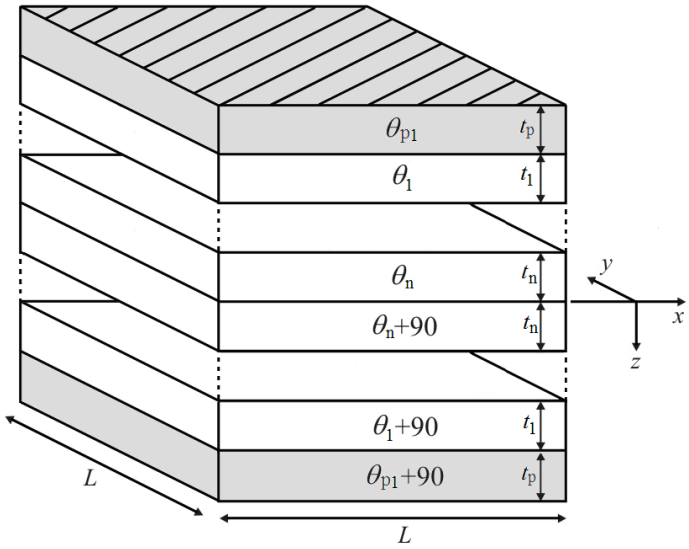

Figure 2. *n*-ply laminate geometry with piezoelectric layers on top and bottom surfaces

We note that the above configuration leads to a number of simplifications to the analytical model. The first simplification relates to the computation of the in-plane (A), coupling (B) and flexural (D) stiffness matrices. Of the 18 terms of the symmetric matrices only 10 need to be calculated to model the problem due to the orthogonality of the layups (Betts, Kim and Bowen, 2011). The plate constitutive equations can therefore be expressed in the following simplified form.

$$\begin{bmatrix} N_x \\ N_y \\ N_{xy} \\ M_x \\ M_y \\ M_{xy} \end{bmatrix} = \begin{bmatrix} A_{11} & A_{12} & A_{16} & B_{11} & 0 & B_{16} \\ A_{12} & A_{11} & -A_{16} & 0 & -B_{11} & B_{16} \\ A_{16} & -A_{16} & A_{66} & B_{16} & B_{16} & 0 \\ B_{11} & 0 & B_{16} & D_{11} & D_{12} & D_{16} \\ 0 & -B_{11} & B_{16} & D_{12} & D_{11} & D_{16} \\ B_{16} & B_{16} & 0 & D_{16} & D_{16} & D_{66} \end{bmatrix} \begin{bmatrix} \varepsilon_x^0 \\ \varepsilon_y^0 \\ \varepsilon_{xy}^0 \\ a \\ b \\ c \end{bmatrix} \tag{1}$$

Secondly, this also simplifies the thermally induced forces, N_{xT}, N_{yT} and N_{xyT}, and thermally induced moments, M_{xT}, M_{yT} and M_{xyT}. For this family of laminates the number of distinct force and moment terms can also be reduced by the following relationships.

$$N_{xT} = N_{yT}, \quad N_{xyT} = 0, \quad M_{xT} = -M_{yT} \tag{2}$$

A. Optimization problem formulation

The optimization problem formulation is defined as follows:

Maximize:	Bending stiffness in a chosen direction, ϕ_1, see Figure 3.
Subject to:	The laminate must be bistable.
	The deflection between states must be greater than a minimum value, representing a significant shape change.
	Reversible snap-through must be within the working voltage limits of the piezoelectric layers.
Variables:	Ply orientations θ_1 and θ_2 defining all four ply orientations.
	Piezoelectric fiber orientation θ_{p1}.
	Laminate geometry defined by ply thicknesses t_1 and t_2, and edge length L.
	Loading direction ϕ_1 and snap-through direction ϕ_2.

B. Objective function

One of the primary concerns associated with the use of bistable laminates for adaptive structures is the inherent flexibility of thin composite plates. The objective function thus, maximizes the stiffness in a chosen direction ϕ_1, defined by the direction of normal operating loads, see Figure 3.

Noting that the out-of-plane displacement, w, in the z-direction is assumed to be of the form of the quadratic polynomial of Equation (3),

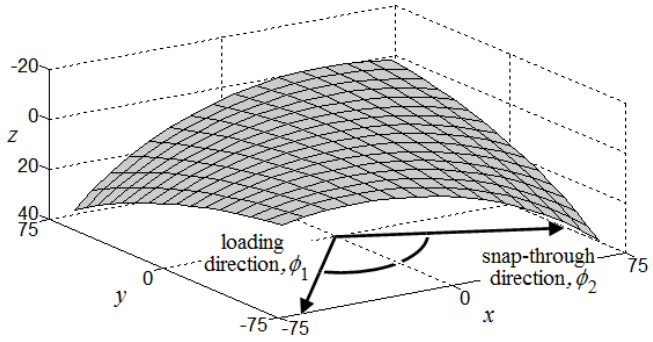

Figure 3. Loading direction ϕ_1 and snap-through direction ϕ_2

$$w(x,y) = 0.5(ax^2 + by^2 + cxy) \tag{3}$$

we characterize the bending stiffness by the change in the curvature in the ϕ_1 direction, a_ϕ, with moment applied in that direction, $M_{x\phi}$, Equation (4).

$$\text{Objective Function} = \frac{\delta a_\phi}{\delta M_{x\phi}} \tag{4}$$

To approximate $\delta a_\phi / \delta M_{x\phi}$ we first transform Equation (1) to align with ϕ_1 rather than the global axes. The forces N_x, N_y and N_{xy}, and moments M_y and M_{xy} are then set to zero. The six equations can then be solved simultaneously to find an analytical expression for the curvature coefficient in the ϕ_1 direction, a_ϕ, in terms of A, B, and D matrix terms and for the remaining moment, $M_{x\phi}$, applied in the ϕ_1 direction. Finally, the expression is differentiated with respect to $M_{x\phi}$ analytically to obtain the objective function.

C. Bistability and deflection constraint

The asymmetric nature of the stacking sequence itself does not ensure bistability. When a laminate geometry has an edge length to thickness ratio below a critical value, there exists only a single saddle shaped solution (Jun and Hong, 1990). When this ratio increases above the critical value, the saddle solution becomes unstable and the stable solution bifurcates to the two cylindrical shapes. Close to this bifurcation point the solution is highly sensitive to uncertainties in both material properties and the manufacturing process (Betts et al., 2010). We address these uncertainties by imposing a constraint to move the solution away from the bifurcation point, ensuring bistability. This is achieved by including a constraint on the minimum deflection between the two stable states (Betts, Kim and Bowen, 2011).

We define the deflection as the change in out-of-plane displacement at a corner of the laminate between the two states. For laminates of this family, the deflections at all corners are equal.

As the out-of-plane displacement, w, is represented by a quadratic polynomial, Equation (3), the corner deflection between states, w_{def}, at $x = y = L/2$ can be expressed by Equation (5), where the subscript denotes the associated stable state.

$$w_{def} = w_1 - w_2 = 0.125(a_1 + b_1 + c_1)L^2 - 0.125(a_2 + b_2 + c_2)L^2 \tag{5}$$

The curvatures a, b and c can be expressed in terms of the first state alone due to the two states having curvatures of equal and opposite magnitude (as in Figure 1). The x- and y-curvatures of the two states switch alignment and out-of-plane direction, while the x-y curvature remains unchanged between states. Equation (5) can therefore be rewritten in terms of only a_1 and b_1, Equation (6), which is then used to define the constraint on minimum deflection between states.

$$w_{def} = 0.25(a_1 + b_1)L^2 \tag{6}$$

D. Actuation constraint

For practical design the laminate must be actuated within the working voltage limits of the piezoelectric layers. We therefore constrain the applied voltage to the piezoelectric layers in the direction of actuation, ϕ_2, to be within these bounds. For the piezoelectric material used in this work, M8557-P1, the lower and upper bounds for applied voltage are -500V and 1500V respectively (Giddings et al., 2011), corresponding to maximum free strain of -450μstrain and 1350μstrain.

III. Analytical Modeling

A. Unloaded laminate shapes

The existing analytical model for the unloaded shapes of asymmetric laminates of arbitrary layup is a nonlinear extension to classical laminated plate theory (Dano and Hyer, 1998). The co-ordinate system used is that defined in Figure 1, where the geometric centre of the laminate sits at the origin. The out-of-plane displacement in the *z*-direction, *w*, is assumed to be of the form of Equation (3). The midplane strains, including geometrical nonlinearity according to the von Karman hypothesis, are defined as

$$\begin{aligned}\varepsilon_x^0 &= \frac{\partial u^0}{\partial x} + \frac{1}{2}\left(\frac{\partial w}{\partial x}\right)^2 \\ \varepsilon_y^0 &= \frac{\partial v^0}{\partial y} + \frac{1}{2}\left(\frac{\partial w}{\partial y}\right)^2 \\ \varepsilon_{xy}^0 &= \frac{\partial u^0}{\partial y} + \frac{\partial v^0}{\partial x} + \frac{1}{2}\frac{\partial w}{\partial x}\frac{\partial w}{\partial y}\end{aligned} \tag{7}$$

where u^0 and v^0 are the in-plane displacements in the *x*- and *y*-directions respectively. The midplane strains are approximated by third order polynomials. Dano and Hyer (1998) considered the complete third order polynomials and found that terms with powers of *x* and *y* that sum to an odd number are always zero. Furthermore, Betts, Kim and Bowen (2011) found that for the family of laminates considered in this paper the polynomials can be further reduced due to the orthogonality of the design. Therefore the form of the midplane strains can be reduced to the polynomials of Equation (8).

$$\begin{aligned}\varepsilon_x^0 &= d_1 + d_2x^2 + d_3xy + d_4y^2 \\ \varepsilon_y^0 &= d_5 + d_4x^2 - d_3xy + d_2y^2\end{aligned} \tag{8}$$

Using Equations (3), (7) and (8) and introducing the additional shape coefficients $d_{6\text{-}8}$ resulting from integration of the midplane strains, expressions for the in-plane displacements u^0 and v^0 can be determined.

$$\begin{aligned}u^0(x,y) &= d_1x + d_6y + \frac{1}{2}\left(d_3 - \frac{1}{2}ac\right)x^2y + \left(d_4 - \frac{c^2}{8}\right)xy^2 + \frac{1}{3}\left(d_2 - \frac{1}{2}a^2\right)x^3 + \frac{1}{3}d_8y^3 \\ v^0(x,y) &= d_6x + d_5y - \frac{1}{2}\left(d_3 + \frac{1}{2}bc\right)xy^2 + \left(d_4 - \frac{c^2}{8}\right)x^2y + \frac{1}{3}\left(d_2 - \frac{1}{2}b^2\right)y^3 + \frac{1}{3}d_7x^3\end{aligned} \tag{9}$$

The total strain energy of the laminate, *W*, can then be expressed as the integral of strain energy density over the volume of the laminate.

$$\int_{-L_x/2}^{L_x/2}\int_{-L_y/2}^{L_y/2}\int_{-H/2}^{H/2}\frac{1}{2}c_{ijkl}\varepsilon_{ij}\varepsilon_{kl} - \hat{\alpha}_{ij}\varepsilon_{ij}\Delta T\,dx\,dy\,dz \tag{10}$$

where c_{ijkl}'s are elastic constants, $\hat{\alpha}_{ij}$'s are constants relating to the thermal expansion coefficients, L_x and L_y are the planform side lengths of the laminate, H is the total laminate thickness, ΔT is the temperature change from cure and ε_{ij}'s and ε_{kl}'s are the total strains defined as

$$\begin{aligned} \varepsilon_x &= \varepsilon_x^0 - za \\ \varepsilon_y &= \varepsilon_y^0 - zb \\ \varepsilon_{xy} &= \varepsilon_{xy}^0 - zc \end{aligned} \tag{11}$$

Expansion of Equation (10) results in an expression for the total energy which is a function of the material and geometric properties, the temperature change from the cure cycle and the set of shape coefficients a, b, c, $d_1 \ldots d_8$. For equilibrium, the minimum energy states require:

$$f_i = \frac{\partial W}{\partial e_i} = 0; \quad i = 1 \ldots 11 \tag{12}$$

where e_i's are the shape coefficients a, b, c, $d_1 \ldots d_8$. This results in 11 nonlinear equations to be solved to find the unloaded stable shapes which are commonly solved using an iterative method such as Newton-Raphson. However, due to the simplifications made in this section based on the design of Figure 2, an analytical solution to Equation (12) can be derived (Betts, Kim and Bowen, 2011). This allows fast and robust analysis of unloaded laminate shapes, thus enabling optimization.

This analytical solution is obtained by first breaking down Equation (12) into its component parts, namely the stiffness matrix terms, thermal loads and moments, shape coefficients and laminate edge length terms. The equilibrium equations can therefore be expressed in the following form

$$f_i = [U][Z][K][T][P]_i[L]; \quad i = 1 \ldots 11 \tag{13}$$

where

$[U]$ = Material stiffness properties
$[Z]$ = Ply orientations
$[K]$ = Material thermal expansion properties
$[T]$ = Ply thickness terms
$[P]_i$ = Shape coefficients
$[L]$ = Laminate edge length terms

The first four terms of Equation (13) are the same for all 11 equations and define the simplified A, B, and D terms of Equation (1), and the reduced number of thermal loads and moments of Equation (2).

$$[U][Z][K][T] = \lfloor A_{11} \;\; A_{12} \;\; A_{16} \;\; A_{66} \;\; B_{11} \;\; B_{16} \;\; D_{11} \;\; D_{12} \;\; D_{16} \;\; D_{66} \;\; N_{xT} \;\; M_{xT} \;\; M_{xyT} \rfloor \tag{14}$$

In this paper we add the effects of the piezoelectric layers. The total contribution of the stiffness matrix terms and forces and moments including the piezoelectric layers, S_{tot}, can therefore be expressed as the following sum,

$$[S_{tot}] = [U][Z][K][T] + [Up][Zp][Kp][Tp] \tag{15}$$

where

$[Up]$ = Piezoelectric stiffness properties
$[Zp]$ = Piezoelectric layer orientations
$[Kp]$ = Piezoelectric thermal expansion properties
$[Tp]$ = Piezoelectric layer thickness terms

As the piezoelectric layers are typically attached post-cure (Schultz, Wilkie and Bryant, 2007; Ren, 2008) they do not produce any thermal forces or moments but do contribute to the *A*, *B* and *D* terms. Equation (15) can then be substituted into Equation (13) to obtain the equilibrium equations for the total laminate including the stiffness contribution of the piezoelectric layers.

$$f_i = [S]_{tot}[P]_i[L]; \quad i = 1...11 \tag{16}$$

Finally, analytical expressions (Betts, Kim and Bowen, 2011) are derived for the out-of-plane displacement coefficients *a*, *b*, and *c*, which are used to define the optimization deflection constraint.

B. Snap-through voltage prediction

To satisfy the actuation constraint, it is necessary to find the actuation voltage at every optimization iteration. To include an applied voltage, the strain energy density of Equation (10) must include an additional piezoelectric term

$$\frac{1}{2}c_{ijkl}\varepsilon_{ij}\varepsilon_{kl} - \hat{\alpha}_{ij}\varepsilon_{ij}\Delta T - \hat{\beta}_{ij}\varepsilon_{ij}\Delta V \tag{17}$$

where $\hat{\beta}_{ij}$'s are constants relating to the piezoelectric coefficients, and ΔV is the change in applied voltage. Expansion of Equation (10) including this additional term results in a set of equilibrium equations which can be solved by Newton-Raphson method for the loaded laminate shapes. Figure 4 illustrates the change in major and minor out-of-plane displacement coefficients, *a* and *b*, with applied voltage for a $[0/90/0^{Piezo}]_T$ laminate. We first compute the exact unloaded, zero-voltage shape at A in Figure 4 using the method outlined in Section III A. Starting at point A, the laminate is in State 1 with large positive coefficient *a*. As the applied voltage is incrementally increased the loaded shapes are computed using the Newton-Raphson method. At a critical voltage, point B, *a* switches to near-zero and the coefficient *b* jumps to a large negative value, point C. The voltage at this transition from point B to C is the snap-through voltage. As the voltage is then incrementally removed, the curvatures approach the unloaded State 2 at point D.

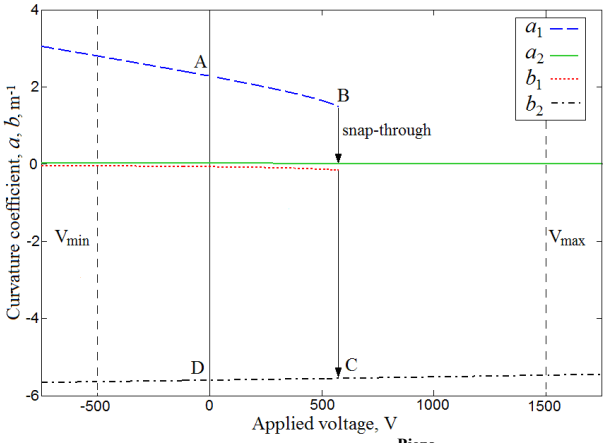

Figure 4. Actuation of a $[0/90/0^{Piezo}]_T$ laminate

IV. Numerical Results

This section presents the results of numerical optimization. We solve the optimization problem using MATLAB's sequential quadratic programming, fmincon. In order to find all optima solutions, we use multiple starting points. All examples use M21/T800 material properties for the laminate and M8557-P1 properties for the piezoelectric layers (Giddings et al., 2011).

A. Maximization of bending stiffness

To demonstrate the nature of the design space we first present optimum solutions constrained only by the orthogonal design rules of Figure 2 and no bistability, deflection or snap-through constraints. The design variables are restricted to the ply orientations for illustration purposes. The square laminate edge length *L* is set to 0.15m which has been examined by a number of researchers (Betts et al., 2010; Betts, Kim and Bowen, 2011; Giddings et al., 2011), and the uniform single ply thickness $t_1 = t_2$ set to 0.1mm. The piezoelectric layers are assumed to have the same edge length *L* with a thickness of 0.2mm. The snap-through direction, ϕ_2, is fixed to 0˚. The pattern of results we observe is dependent on the relative values of the snap-through direction and loading direction rather than the individual angles. Figure 5 shows the design space for this problem for changing values of the loading direction, ϕ_1. The contours show the objective function value, the black dots are used to indicate points where Equation (4) is locally optimal and white dots are used to indicate global optima.

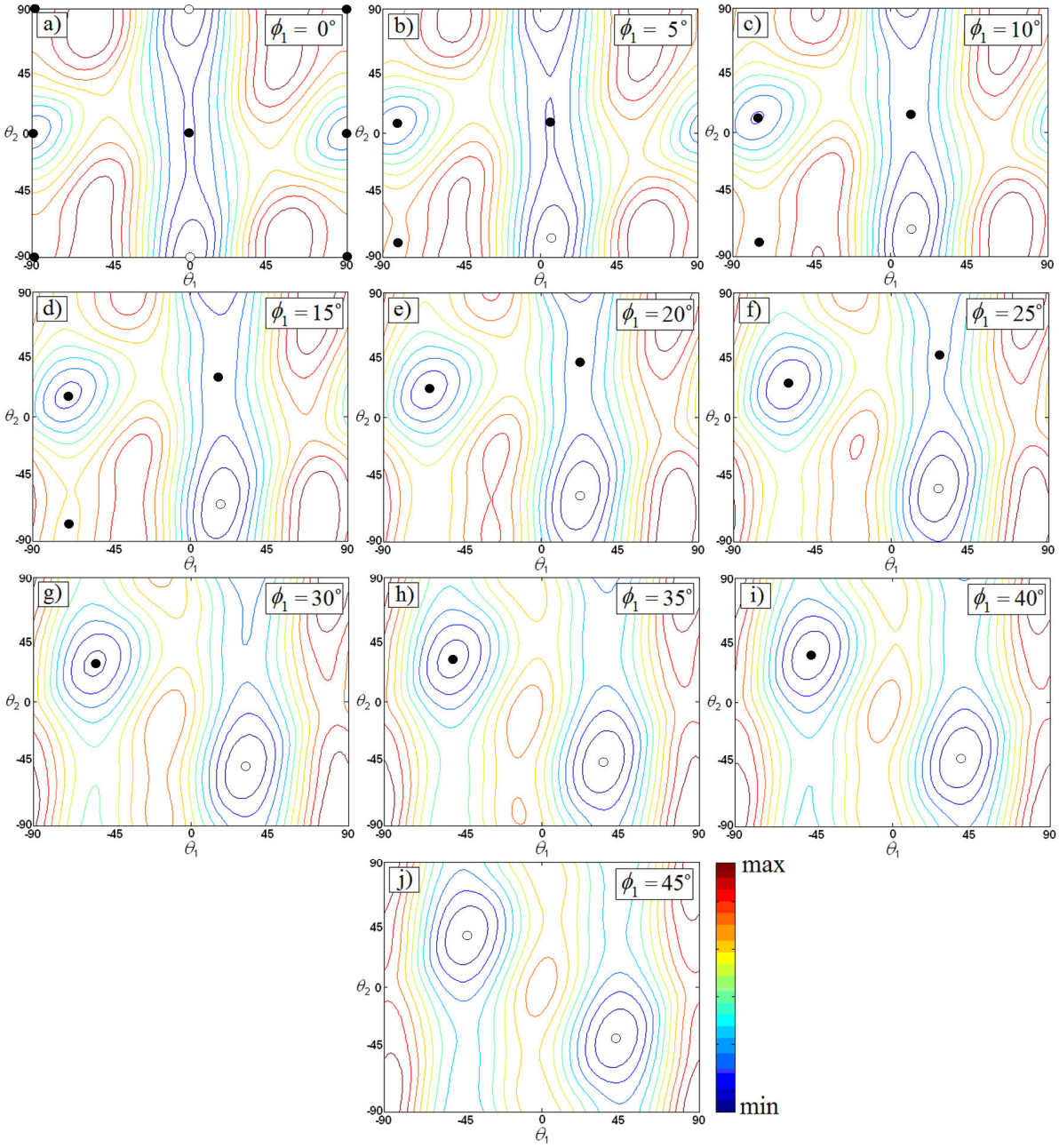

Figure 5. Variation in design space for a [0^{Piezo}/θ_1/θ_2/θ_2+90/θ_1+90/90^{Piezo}] laminate, contours representing the objective function, with change in loading direction, ϕ_1.

With the loading direction initially set to 0˚, four distinct local solutions are found for laminates of [0/0/90/90], [90/90/0/0], [0/90/0/90] and [90/0/90/0], Figure 5a. Due to the periodic nature of the design space these solutions are repeated at equivalent positions along the boundaries of the design space. Each of these four solutions has a different value of the objective function, with the global optimum found at [0/90/0/90] with a value of 0.737. As the loading direction, ϕ_1, is changed the pattern of four local solutions is shifted away from 0˚ and 90˚ ply angles and the solutions no longer appear orthogonally to one another. When ϕ_1 approaches 20˚ one of the four solutions is lost. Of the remaining three solutions the global optimum is found at [22/-58/32/-68] with a value of 0.811, Figure 5e. When ϕ_1 = 30º, the number of local solutions reduces further to just two, Figure 5g. As ϕ_1 tends towards 45º the two remaining solutions become closer to being orthogonal to one another until settling on [44/-38/52/-46] and [-44/38/-52/46] at ϕ_1 = 45º, with both solutions exhibiting equal objective function value of 0.936, Figure 5j.

In addition to the changing number of optimum solutions, we observe an increase in the global optimum objective function values with increasing ϕ_1. Figure 6 shows this relationship for the range of ϕ_1. The minimum solution is found when ϕ_1 is 0º. This design represents a laminate layup where the piezoelectric layer orientations are orthogonal to the chosen loading direction. This is expected as the laminate composition makes best use of the directional stiffnesses of composite materials by having the two conflicting stiffness requirements as far apart as possible.

For comparison, the optimum cross-ply solutions, $[\theta_1/\theta_1/\theta_1+90/\theta_1+90]$ are also shown in Figure 6. Comparing these solutions against the global optima reveals improvement in objective function from 12% to 29% is obtained by the use of ply orientations as defined by design rule 2.

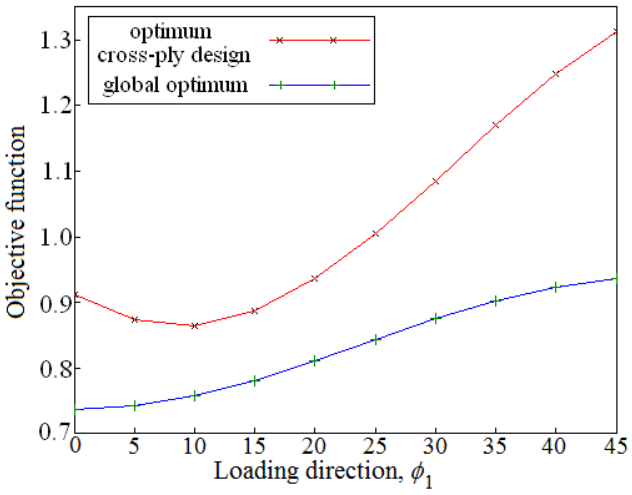

Figure 6. Variation in objective function with change in loading direction

B. Addition of deflection and actuation constraints

This section investigates how the optimum solutions are affected by the introduction of a minimum deflection and actuation voltage constraints. Figure 7 shows contours of the deflection between two states for the geometry outlined in the previous section, where the edge length L is 0.15m, ply thickness t is 0.1mm and the piezoelectric layers are oriented at 0º and 90º. The peak deflection is observed at the centre of Figure 7. This composite laminate geometry is bistable for all ply orientations considered as the edge length to thickness ratio is sufficiently high. In the unconstrained examples it was observed that the global optimum stiffness solutions tend to sit in the regions marked by the solid black lines in Figure 7, while the highest deflection designs are observed in the region marked by the dashed line. This conflict demonstrates the need for constrained optimization to tailor the design.

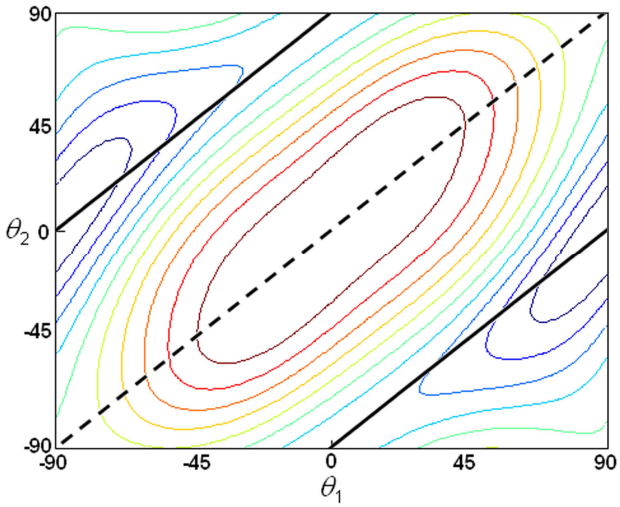

Figure 7. Deflection between states for a $[0^{Piezo}/\theta_1/\theta_2/\theta_2+90/\theta_1+90/90^{Piezo}]_T$ laminate

The deflection and actuation (from -500V to 1500V) constraints are now introduced for a range of loading directions (0˚ to 45˚ at 5˚ intervals) and a fixed snap-through direction (0˚) as in the unconstrained examples. Application of a positive voltage to the piezoelectric layer leads to an expansion, while a negative potential leads to a contraction. The maximum positive voltage of 1500V represents a limit to avoid dielectric breakdown of the piezoelectric and corresponds to a free strain of 1350μstrain. The -500V cannot be exceeded since it can lead to depolarization of the piezoelectric and corresponds to a free strain of -450μstrain. The design variables include the non-uniform ply thicknesses t_1 and t_2 and laminate edge length L as well as the ply orientations. However, all locally optimum designs for this problem are found at the upper or lower bounds of the geometric variables. We therefore present results with the square laminate edge length set to 0.15m, and the uniform single ply thickness set to 0.1mm, noting that an increase in edge length or a decrease in ply thickness will increase the achievable deflection but not affect the general pattern of results observed.

Figure 8 shows the constrained design space for three example loading directions, 0º, 20º, and 45º, chosen to show the behavior across the range shown in Figure 5. For each loading direction we present the results for the snap-through voltage constrained by the upper limit of the working range, 1500V, where the infeasible region is marked in light grey. Each example is repeated for a range of deflection constraint values (30-70mm at 10mm intervals, 30, 50 and 70mm shown in Figure 8), with the infeasible regions marked in dark grey. The local solutions are marked with black dots, and the global solutions are marked with white dots.

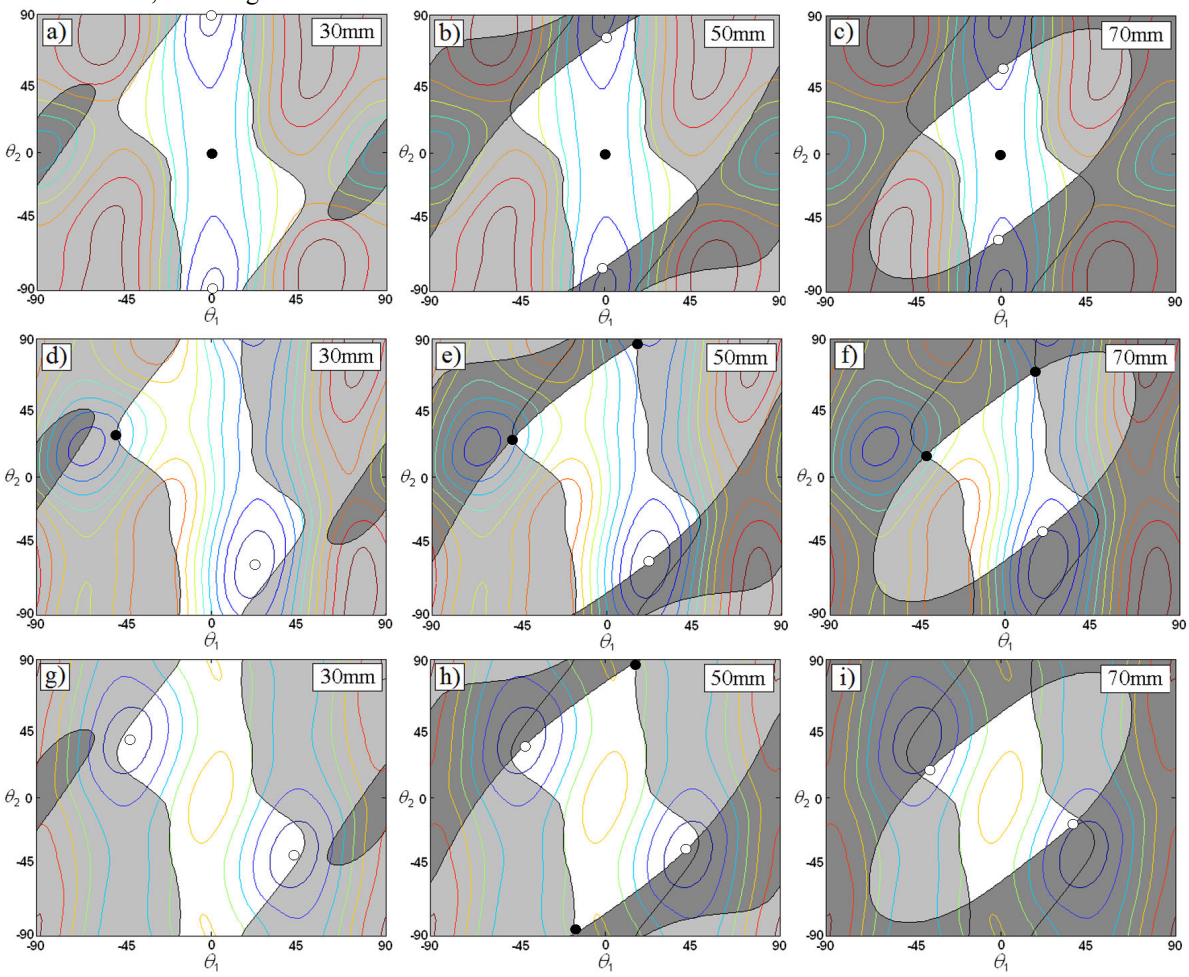

Figure 8. Constrained design for loading directions a-c) ϕ_1 = 0º, d-f) ϕ_1 = 20º and g-i) ϕ_1 = 45º, for different deflection constraint values of 30, 50, and 70mm. Light grey regions infeasible due to voltage constraint, dark grey regions infeasble due to deflection constraint

The global optimum solutions are summarized in Table 1. We see in Figure 8a that the global optimum solution for 0º loading direction and the deflection constraint of 30mm is not affected by the constraints. Some local solutions are found to be infeasible, but [0/90/0/90] is still the global optimum with a value of 0.737. As the deflection constraint is increased to 50mm this solution becomes infeasible and a new global optimum is found on the deflection constraint boundary at [2/76/-14/-88] with an increased value of 0.754, Figure 8b. Increasing the deflection constraint further to 70mm continues to move the solution away from the unconstrained optimum. The actuation constraint (light grey region) remains inactive for all deflection values in Figures 8a-c.

For the solutions with loading direction of 20º a similar pattern is observed (Figures 8d-f). For the low deflection constraint of 30mm the global optimum is unchanged, [22/-59/31/-68] with a value of 0.811, Figure 8d. An additional local solution is found where the actuation constraint is active. As the deflection requirement is increased from 30mm to 50mm the global solution is shifted by the deflection constraint boundary to [21/-56/34/-69] with a value of 0.813 and an additional local solution constrained by the actuation requirement appears, Figure 8e.

Finally, for the loading direction at 45º we see a slight change in the pattern of the optimum solutions (Figures 8g-i). Due to the symmetry of this particular problem we find two solutions of equal objective value. For the 30mm

deflection problem these solutions are unconstrained and are found at [43/-38/52/-47] and [-43/38/-52/47] with a value of 0.936, Figure 8g. As the deflection constraint is increased these two solutions move simultaneously to points on the constraint boundary, still with equal but higher objective value (Figures 8h and 8i). In all cases, the light grey actuation constraint remains inactive for the global optima.

These examples demonstrate that actuation through the use of two orthogonal piezoelectric layers is achievable for this family of laminates. Furthermore the state-change is achievable while maintaining a useful deflection between states and a reasonable improvement on the typical high deflection cross-ply designs, as shown in Figure 6.

Table 1: Global optimum solutions

Loading direction (ϕ°)	Deflection constraint (mm)	First ply angle (θ°)	Second ply angle (θ°)	Actual deflection (mm)	Objective function
0	30	0	90	43.3	0.737
	40	0	90	43.3	0.737
	50	2	76	50.0	0.754
	60	4	68	60.0	0.773
	70	2	56	70.0	0.787
20	30	22	-59	46.7	0.811
	40	22	-59	46.7	0.811
	50	21	-56	50.0	0.813
	60	21	-44	60.0	0.832
	70	20	-36	70.0	0.854
45	30	43	-38	44.2	0.936
	40	43	-38	44.2	0.936
	50	41	-33	50.0	0.943
	60	39	-25	60.0	0.972
	70	36	-19	70.0	1.014

In all examples examined in this paper the actuation voltage constraint was not the constraining factor for the global optimum designs. This problem formulation also makes use of only one of the piezoelectric layers at any one time with the second piezoelectric layer used for the reverse actuation. Given that we do not use the full capacity of the actuation and neglect the potential of the second layer to contract under the application of a negative bias there is scope for a reduction in the total voltage requirement.

C. Combined use of two piezoelectric layers

The piezoelectric layers modeled in this work have a working range of -500V to 1500V. However, frequent use at these high voltage levels can lead to degradation of the piezoelectric and a reduced lifespan (Pritchard, Bowen and Lowrie, 2001; Hooker et al., 2007). Furthermore the use of drive voltages in excess of 1000V may limit application of the technology due to safety concerns or the need to rectify local power sources. Having considered only the use of the positive range of one piezoelectric layer so far, and having shown that this constraint is not active at the global optima for all cases, we investigate whether the actuation voltage requirement can be reduced by simultaneously utilizing the negative voltage range of the layer on the opposite laminate surface.

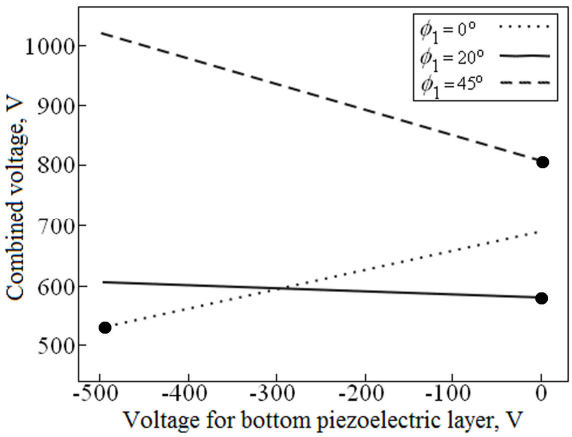

Figure 9. Combined voltage requirements for 50mm deflection

We first analyze the voltage requirement for each optimum stiffness solution shown in Table 1. Figure 9 shows the variation in the total voltage requirement (top layer voltage + bottom layer voltage) for each loading direction for the 50mm deflection problem. The black dots indicate the lowest combination of voltages for each example. For the 45˚ loading direction the optimum solution is found when the bottom layer voltage is 0V. We therefore find no improvement in the voltage requirement. For the 20˚ loading direction we again find the optimum solution is to use only the positive range of the top layer. However,

the increase in combined voltage with increase in negative voltage is more gradual. For the 0˚ loading direction this pattern is reversed, with the optimum combination found at the negative voltage limit, -500V. This is combined with a small positive voltage of 30V for the opposite layer. The combined requirement of 530V represents a 23.7% reduction on the total applied voltage using only one piezoeletric layer. Results for all cases are shown in Table 2.

We find that a reduction in the total voltage requirement is achievable for the 0˚ loading direction with up to 33.8% reduction from the corresponding single layer actuation solutions. In the case of a 40mm deflection constraint, $[0^{Piezo}/0/90/0/90/90^{Piezo}]$, we see that using a negative voltage input on the bottom layer without the top layer actuation requires less voltage input. For the 20˚ loading direction there is a clear switching point where the use of the bottom layer no longer aids actuation. This is also the case for all 45˚ loading direction cases. Whether the bottom layer actuation is effective is dependent on the orientation of the piezoelectric layers relative to the laminate major curvature.

Table 2: Voltage requirements using both piezoelectric layers simultaneously

Loading direction (ϕ˚)	Deflection constraint (mm)	Top layer (V)	Bottom layer (V)	Combined voltage (V)	Reduction (%)
0	40	0	-410	410	33.8
	50	30	-500	530	23.7
	60	215	-500	715	11.7
	70	355	-500	855	1.7
20	40	75	-500	575	2.5
	50	590	0	590	0
	60	675	0	675	0
	70	775	0	775	0
45	40	865	0	865	0
	50	815	0	815	0
	60	940	0	940	0
	70	1085	0	1085	0

This study only considered orthogonal piezoelectric layers and showed that the use of both layers simultaneously can reduce the total voltage requirement. This suggests that there is scope for further improvement by relaxing the constraint on the piezoelectric layer orientations and making use of the full working range of the layers.

V. Conclusion

This paper presents an optimization study for the design of reversibly actuated bistable orthogonal laminates. This class of laminates have been chosen to allow tailoring of the directional stiffness whilst offering maximum useful deflection between states. The optimization study has been enabled by the incorporation of two orthogonal piezoelectric layers into an existing analytical solution for the shapes of bistable laminates. We use the objective function to maximize the bending stiffness of the laminates in a chosen loading direction. Two constraints are imposed: minimum deflection and the voltage applied to the piezoelectric layers. With the ply orientations and laminate geometry as variables we find the optimization problem to be multimodal, with the interactions of the multiple local optima with the constraint boundaries dependent on the chosen loading and snap-through directions and the values of the constraints. We use a sequential quadratic programming method to solve the optimization problem. Given the complex and multimodal nature of the actuated bistable laminate design problem, multiple starting points are required to capture all local optima.

We use the optimization tool to investigate the total voltage requirements. Through the combined use of the positive and negative applied voltages to the top and bottom piezoelectric layers, we find that a reduction in the total actuation voltage of up to 33.8% is achievable in some cases.

References

Betts, D.N. Kim, H.A. and Bowen, C.R., 2011 "Design optimization of stiffness characteristics for bistable composite laminates," 52nd AIAA/ASME/ASCE/AHS/ASC Structures, Structural Dynamics and Materials Conference, AIAA, Denver CO.

Betts, D.N. Salo, A.I.T. Bowen, C.R. and Kim, H.A., 2010 "Characterisation and modelling of the cured shapes of arbitrary layup bistable composite laminates," Composite Structures, 92(7):1694-1700, (doi:10.1016/j.compstruct.2009.12.005).

Dang, J. and Tang, Y., 1986 "Calculation of the room-temperature shapes of unsymmetric laminates," Proceedings of the International Symposium on Composite Materials and Structures, 201-206, Technomic Publishing, Lancaster, PA.

Dano, M.-L. and Hyer, M.W., 1996 "The response of unsymmetric laminates to simple applied forces," Mechanics of Composite Materials and Structures, 3(1):65-80, (doi:10.1080/10759419608945854).

Dano, M.-L. and Hyer, M.W., 1998 "Thermally induced deformation behavior of unsymmetric laminates," International Journal of Solids and Structures, 35(17):2101-2120, (doi:10.1016/S0020-7683(97)00167-4).

Dano, M.-L. and Hyer, M.W., 2003 "SMA-induced snap-through of unsymmetric fiber-reinforced composite laminates," International Journal of Solids and Structures, 40(22):5949-5972, (doi:10.1016/S0020-7683(03)00374-3).

Giddings, P.F. Kim, H.A. Salo, A.I.T. and Bowen, C.R., 2011 "Modelling of piezoelectrically actuated bistable composites," Materials Letters, 65(9):1261-1263, (doi:10.1016/j.matlet.2011.01.015).

Hooker, S. Mueller, J. Kostelecky, C. and Womer, K., 2007 "Fatigure resistant miniature piezoceramic actuators," Journal of Intelligent Material Systems and Structures, 18(2):153-157, (doi:10.1177/1045389X06063460).

Hufenbach, W. Gude, M. and Kroll, L., 2002 "Design of multistable composites for application in adaptive structures," Composites Science and Technology, 62(16):2201-2207, (doi:10.1016/S0266-3538(02)00159-8).

Jun, W.J. and Hong, C.S., 1990 "Effect of residual shear strain on the cured shape of unsymmetric cross-ply laminates," Composite Science and Technology, 38(1):55-67, (doi:10.1016/0266-3538(90)90071-C).

Kim, H.A. Betts, D.N. Salo, A.I.T. and Bowen, C.R., 2010 "Shape memory alloy – piezoelectric active structures for reversible actuation of bistable composites," AIAA Journal, 48(6):1265-1268, (doi:10.2514/1.J050100).

Pritchard, J. Bowen, C.R. and Lowrie, F., 2001 "Multilayer actuators: review," British Ceramic Transactions, 100(6):265-273, (doi:10.1179/096797801681549).

Ren, L.B., 2008 "A theoretical study on shape control of arbitrary lay-up laminates using piezoelectric actuators," Composite Structures, 83(1):110-118, (doi:10.1016/j.compstruct.2007.10.030).

Schultz, M.R. Wilkie, W.K. and Bryant, R.G., 2007 "Investigation of self-resetting active multistable laminates," Journal of Aircraft, 44(4):1069-1076, (doi:10.2514/1.17404).